https://doi.org/10.1093/brain/awac004 BRAIN 2022: 145; 3571–3581 | 3571

BRAIN
ORIGINAL ARTICLE

Genetically identical twins show comparable tau PET load and spatial distribution

Emma M. Coomans,[1,2] Jori Tomassen,[2] Rik Ossenkoppele,[2,3] Sandeep S. V. Golla,[1] Marijke den Hollander,[1] Lyduine E. Collij,[1] Emma Weltings,[1] Sophie M. van der Landen,[2] Emma E. Wolters,[1] Albert D. Windhorst,[1] Frederik Barkhof,[1,4] Eco J.C. de Geus,[5] Philip Scheltens,[2] Pieter Jelle Visser,[2,6,7] Bart N. M. van Berckel[1] and Anouk den Braber[2,5]

Tau accumulation starts during the preclinical phase of Alzheimer's disease and is closely associated with cognitive decline. For preventive purposes, it is important to identify factors associated with tau accumulation and spread. Studying genetically identical twin-pairs may give insight into genetic and environmental contributions to tau pathology, as similarities in identical twin-pairs largely result from genetic factors, while differences in identical twin-pairs can largely be attributed to non-shared, environmental factors. This study aimed to examine similarities and dissimilarities in a cohort of genetically identical older twin-pairs in (i) tau load; and (ii) spatial distribution of tau, measured with ^{18}F-flortaucipir PET.

We selected 78 genetically identical twins (39 pairs; average age 73 ± 6 years), enriched for amyloid-β pathology and *APOE* ϵ4 carriership, who underwent dynamic ^{18}F-flortaucipir PET. We extracted binding potentials (BP_{ND}) in entorhinal, temporal, widespread neocortical and global regions, and examined within-pair similarities in BP_{ND} using age and sex corrected intra-class correlations. Furthermore, we tested whether twin-pairs showed a more similar spatial ^{18}F-flortaucipir distribution compared to non-twin pairs, and whether the participant's co-twin could be identified solely based on the spatial ^{18}F-flortaucipir distribution. Last, we explored whether environmental (e.g. physical activity, obesity) factors could explain observed differences in twins of a pair in ^{18}F-flortaucipir BP_{ND}.

On visual inspection, Alzheimer's disease-like ^{18}F-flortaucipir PET patterns were observed, and although we mainly identified similarities in twin-pairs, some pairs showed strong dissimilarities. ^{18}F-flortaucipir BP_{ND} was correlated in twins in the entorhinal ($r = 0.40$; $P = 0.01$), neocortical ($r = 0.59$; $P < 0.01$) and global ($r = 0.56$; $P < 0.01$) regions, but not in the temporal region ($r = 0.20$; $P = 0.10$). The ^{18}F-flortaucipir distribution pattern was significantly more similar between twins of the same pair [mean $r = 0.27$; standard deviation (SD) = 0.09] than between non-twin pairings of participants (mean $r = 0.01$; SD = 0.10) ($P < 0.01$), also after correcting for proxies of off-target binding. Based on the spatial ^{18}F-flortaucipir distribution, we could identify with an accuracy of 86% which twins belonged to the same pair. Finally, within-pair differences in ^{18}F-flortaucipir BP_{ND} were associated with within-pair differences in depressive symptoms ($0.37 < \beta < 0.56$), physical activity ($-0.41 < \beta < -0.42$) and social activity ($-0.32 < \beta < -0.36$) (all $P < 0.05$).

Overall, identical twin-pairs were comparable in tau load and spatial distribution, highlighting the important role of genetic factors in the accumulation and spreading of tau pathology. Considering also the presence of dissimilarities in tau pathology in identical twin-pairs, our results additionally support a role for (potentially modifiable) environmental factors in the onset of Alzheimer's disease pathological processes, which may be of interest for future prevention strategies.

1 Department of Radiology and Nuclear Medicine, Amsterdam Neuroscience, Vrije Universiteit Amsterdam, Amsterdam UMC, Amsterdam, The Netherlands

Received September 07, 2021. Revised November 05, 2021. Accepted November 26, 2021. Advance access publication January 12, 2022

2 Alzheimer Center Amsterdam, Department of Neurology, Amsterdam Neuroscience, Vrije Universiteit Amsterdam, Amsterdam UMC, Amsterdam, The Netherlands
3 Clinical Memory Research Unit, Lund University, Lund, Sweden
4 UCL Institute of Neurology, London, UK
5 Department of Biological Psychology, Vrije Universiteit Amsterdam, Amsterdam, The Netherlands
6 Alzheimer Center Limburg, School for Mental Health and Neuroscience, Maastricht University, Maastricht, The Netherlands
7 Department of Neurobiology, Care Sciences and Society, Division of Neurogeriatrics, Karolinska Institutet, Stockholm Sweden

Correspondence to: Emma M. Coomans
Department of Radiology and Nuclear Medicine Amsterdam UMC, VUmc PO Box 7057, 1007MB Amsterdam, The Netherlands
E-mail: e.coomans@amsterdamumc.nl

Keywords: Alzheimer's disease; tau; PET; twins; genetics

Introduction

The pathophysiological course of Alzheimer's disease lasts decades and includes a long preclinical phase.[1] Within this preclinical phase, the brain gradually accumulates amyloid-β and tau pathology, while cognitive functioning is still within normal limits.[2–4] Whereas amyloid-β plaques are detectable widespread throughout the brain relatively early in the disease course,[5] the distribution of neurofibrillary tau tangles starts focally and spreads throughout the brain followed by clinical disease progression.[6,7] The neuropathological Braak staging system describes how cortical neurofibrillary tau tangles are first observed in the (trans)entorhinal region of the medial temporal lobe, followed by adjacent limbic and lateral temporal regions and finally the neocortex.[8,9] This stereotypical tau spreading pattern has also been observed in *in vivo* PET studies at group level,[10–12] although deviations from this pattern at the individual level may exist, including patterns of hemispheric asymmetry.[7,13] Studies have shown that both the load and location of neurofibrillary tau tangles are closely associated with cognitive functioning and decline.[14–18] More specifically, the load of tau pathology correlates with symptom severity or disease severity,[16] and the regional localization of tau pathology corresponds to the type of symptoms or disease phenotype.[14,19,20] Also in cognitively unimpaired elderly, subtle declines in cognitive functioning have been associated with tau pathology in mainly medial temporal regions.[15,21–23] For preventive purposes, it is therefore critical to understand which factors contribute to the accumulation onset and regional distribution of tau pathology in the earliest stages of the disease.

Studying genetically identical twins provides an excellent approach to study the contribution of genetic and environmental factors to a trait. As identical twin pairs share the same genetic background, similarities in twins from a pair result from either shared genetic or shared environmental factors, although the influence of shared environmental factors (e.g. being raised in the same family) on brain measures in older twins is typically minimal.[24,25] Dissimilarities in twins from a genetically identical pair will largely result from non-shared environmental factors that are unique to one of the twins. Examining tau pathology in the preclinical Alzheimer's disease phase in identical twins may thereby provide valuable information for clinical trials aimed at prevention strategies.

The aim of this study is to assess to what extent genetic and environmental factors contribute to tau pathology, as measured with ^{18}F-flortaucipir PET, using a cohort of genetically identical older twin pairs enriched for preclinical Alzheimer's disease pathology. In this study, we assessed similarities in twins in two characteristics of tau PET: (i) tau load; and (ii) spatial distribution of tau including hemispheric lateralization. Further, we explored which environmental (e.g. physical activity, smoking or obesity) risk factors were associated with observed differences in tau pathology, using a within twin-pair differences regression model. As the heritability for Alzheimer's disease dementia is relatively high (i.e. genetic factors explain up to 80% of the variance in Alzheimer's disease dementia),[26] and tau pathology is a key factor in Alzheimer's disease, we hypothesize that large similarities in tau pathology in genetically identical twins will be observed.

Materials and methods

Participants

We selected 80 genetically identical twins from the longitudinal Amsterdam substudy of the EMIF-AD PreclinAD cohort to undergo tau-PET imaging.[27] We selected twin-pairs of whom both twins or either one of the twins were amyloid-β positive (based on baseline ^{18}F-flutemetamol PET visual read[28]) or were classified into a high amyloid-β stage (based on a previously applied staging model to the baseline ^{18}F-flutemetamol PET scans[29]), twin-pairs that carried an *APOE* ε4 allele, as well as age and sex-matched amyloid-β negative twin-pairs. The number of participants per amyloid-β stage are shown in Supplementary Table 1. Tau-PET was performed during the EMIF-AD PreclinAD 4-year follow-up visit, which took place 4.6 ± 0.6 years after the baseline visit. All participants had normal cognition at EMIF-AD PreclinAD study enrolment. Baseline inclusion criteria were age ≥ 60 years, global Clinical Dementia Rating score of 0, with a score of 0 on the memory sub domain,[30] delayed recall score > −1.5 SD of demographics-adjusted normative data on the Consortium to Establish a Registry for Alzheimer's Disease 10-word list,[31] Telephone Interview for Cognitive Status modified score of ≥23 and a 15-item Geriatric Depression Scale score of <11.[32] Baseline exclusion criteria were any significant neurologic, systemic or psychiatric disorder that could cause cognitive impairment. Additional exclusion criteria for tau-PET imaging were significant cerebrovascular disease on MRI (e.g. territorial infarcts) or a history of major traumatic brain injury. Twin zygosity was confirmed at baseline by buccal cell DNA analysis.

For the analyses, we only included complete twin pairs. Singletons (of which the co-twin deceased prior to the 4-year follow-up visit and thus did not undergo tau-PET imaging, $n = 2$ participants) were excluded, resulting in a total of 78 genetically identical twins (39 pairs) included in the analyses.

The Medical Ethics Review Committee of the VU University Medical Center (Amsterdam, The Netherlands) approved this study. All subjects provided written informed consent.

MRI acquisition

Participants underwent 3D T_1-weighted MRI on a 3.0 T Ingenuity TF PET/MR (Philips Medical Systems). All MRI scans were acquired within a maximum of 12 months from the tau-PET scan [median time lag: 0.0 ± 5.9 months, interquartile range (IQR): 3.0 months].

Tau-PET acquisition

Participants underwent dual time point dynamic ^{18}F-flortaucipir (tau) PET on an Ingenuity TF PET/CT (Philips Medical Systems), which was validated in a previous study.[33] ^{18}F-flortaucipir PET data were acquired during the 0–30 min and 80–100 min time interval immediately following injection of 227 ± 56 MBq (injected mass 1.8 ± 1.2 μg). A low-dose CT scan for attenuation correction was made prior to both the first and the second scan. PET data were 3D RAMLA reconstructed with a matrix size of 128 × 128 × 90 and a final voxel size of 2 × 2 × 2 mm^3, and corrected for attenuation, scatter, randoms, decay and dead time.

Tau-PET binding potential

Both parts of the dynamic scan were co-registered using Vinci software.[33] The high-resolution T_1-weighted MRI was co-registered to the corresponding PET images in native space using Vinci software. Grey matter regions of interest from the Hammers template[34] and Svarer template[35] were automatically delineated on the co-registered magnetic resonance images and superimposed on the PET scan using PVElab to extract time activity curves. Voxel-wise parametric images of binding potential (BP_{ND}) were generated using receptor parametric mapping with whole cerebellar grey matter from the Hammers template as the reference region.[33,36] PET images were analysed with and without partial volume correction using Van Cittert iterative deconvolution methods combined with highly constrained back-projection.[37] Results from partial volume corrected data were similar and are shown in Supplementary Table 2.

Tau-PET region of interest analyses

For region of interest analyses, subject-space bilateral regions of interest were *a priori* selected, in line with previous studies and corresponding to Braak and Braak stages.[8,10,38] We included the entorhinal cortex as an early-stage tau region (Braak I) obtained from the Svarer template, as this region is not available as a separate region of interest in the Hammers template. We created a temporal composite region of interest as an intermediate-stage tau region (Braak III/IV), which included the amygdala, fusiform, parahippocampal and ambient gyrus and middle and inferior temporal gyrus from the Hammers template. We included a widespread neocortical composite region of interest as a late-stage tau region (Braak V/VI), which included the superior temporal gyrus, insula, lateral occipital lobe, cinguli anterior, cinguli posterior, middle frontal, posterior temporal, inferolateral parietal, gyrus rectus, orbitofrontal gyrus, inferior frontal gyrus, superior frontal, superior parietal, lingual gyrus, cuneus, precentral and postcentral gyrus from the Hammers template. Last, a global brain region was created including all regions of interest from the early, intermediate and late tau stage regions combined (i.e. Braak I–VI). The hippocampus was not included in the regions of interest because of possible off-target ^{18}F-flortaucipir spill-in from the adjacent choroid plexus.[39]

For each region of interest, we also calculated a hemispheric lateralization measure (the laterality quotient[40]) using the formula Laterality quotient (%) = 100 × (R − L)/(R + L).[14] This quotient was used to examine how similar twins were in lateralized (asymmetric) ^{18}F-flortaucipir uptake, as a measure for spatial distribution. A negative laterality quotient indicates more tau in the left hemisphere, while a positive laterality quotient indicates more tau in the right hemisphere.

Tau-PET voxel-wise analyses

For voxel-wise analyses, we spatially normalized the parametric PET images to Montreal Neurological Institute (MNI) space using Statistical Parametric Mapping (SPM) version 8 software (Wellcome Trust Centre for Neuroimaging, University College London, UK) by using the transformation matrixes derived from warping the co-registered T_1-weighted MRI scans to MNI space. All warped images were visually checked for transformation errors. We created a group-average image of ^{18}F-flortaucipir BP_{ND} for visualization purposes. Prior to voxel-wise statistical analyses, a cerebral grey matter mask (excluding the basal ganglia because of potential off-target ^{18}F-flortaucipir binding) was applied to the MNI-transformed images. These images were used to assess within-pair similarities in voxel-by-voxel ^{18}F-flortaucipir spatial distribution.

Amyloid-β PET visual read and global binding potential

Participants underwent dynamic ^{18}F-flutemetamol (amyloid-β) PET during the EMIF-AD PreclinAD baseline visit (i.e. 4 years prior to tau-PET) as previously described.[28,41] For stratification analyses, we used baseline amyloid-β status (positive/negative) based on majority visual read of the dynamic ^{18}F-flutemetamol BP_{ND} images.[28] Baseline ^{18}F-flutemetamol BP_{ND} visual read was missing for three participants, for which we used baseline ^{18}F-flutemetamol standardized uptake value ratio (SUVR) visual read ($n = 2$) or ^{18}F-flutemetamol SUVr visual read obtained at time of tau-PET ($n = 1$). Global baseline ^{18}F-flutemetamol BP_{ND}, calculated as previously described,[41] was used as a covariate in further exploratory statistical analyses (missing for $n = 4$ participants).

Environmental risk factors

As differences in identical twin pairs can largely be attributed to non-shared environmental (e.g. physical activity and smoking) factors, we exploratory examined whether within-pair differences in ^{18}F-flortaucipir BP_{ND} were associated with within-pair differences in environmental factors. In line with the Lancet Commission 2020 update on dementia prevention, intervention, and care on potentially modifiable risk factors for late-life cognitive decline,[42] we included proxy variables for (i) less education (years of education); (ii) hearing loss [speech reception threshold (SRT) on the Digit-in-Noise (DIN) test,[43] measuring auditory speech recognition abilities in noise]; (iii) hypertension [average mean arterial pressure (MAP) from three subsequent measurements]; (iv) alcohol (current number of glasses consumed per day); (v) obesity [body mass index (BMI)]; (vi) smoking (number of pack years); (vii) depression [Geriatric Depression Scale (GDS) total score];[32] (viii) social isolation (The Health Related Quality of Life Short Form 12 sub-question: 'Did your health limited your social activities?'); and (ix) physical

inactivity [Physical Activity Scale for the Elderly (PASE) total score].[44] Risk factor variables were assessed within the EMIF-AD PreclinAD study at time of tau-PET imaging. Although listed as potentially modifiable risk factors,[42] we did not include traumatic brain injury (due to it being an exclusion criteria in the current study), air pollution and diabetes (no suitable measures available). Details regarding these questionnaires and measurements are specified in Supplementary Table 3.

Statistical analyses

All statistical analyses were performed in R (R, version 3.6.1, www://R-project.org). A P-value < 0.05 was considered statistically significant.

Similarities in twins in ^{18}F-flortaucipir binding potential

To examine similarities in twins in ^{18}F-flortaucipir BP_{ND} (tau load), we performed one-way single-measure intra-class correlations across twin pairs for each region of interest (i.e. a correlation between Twin 1 and Twin 2 across the group) (Fig. 1A). Because identical twins share the same genetic background, these intra-class correlations provide an estimate of the upper limit of genetic contribution to a trait. We repeated these correlation analyses for 20 different sets (each set consisting of 39 pairs) of random (non-twin) pairs using Pearson correlations. We then determined whether the twin pair correlation coefficient was significantly higher than the average correlation coefficient observed for random pairs using the Fisher-Z-transformation and z-test statistic. This reflects whether twin-pairs are more similar in tau load than what would be observed by chance (i.e. in randomly paired participants). Both the twin pair correlation analyses and the random pair correlation analyses were adjusted for age and sex. We explored the effect of baseline amyloid-β status on the within-pair similarities in ^{18}F-flortaucipir BP_{ND} by stratifying the sample based on twins concordant on amyloid-β status (i.e. both twins of the same pair amyloid-β negative or both twins of the same pair amyloid-β positive) and twins discordant on amyloid-β status (i.e. one twin of the same pair amyloid-β negative and the co-twin amyloid-β positive).

Similarities in twins in spatial distribution of ^{18}F-flortaucipir binding potential

We examined similarities in spatial distribution of ^{18}F-flortaucipir BP_{ND} in twins using three different approaches (all adjusted for age and sex). First, we assessed within-pair similarities in regional hemispheric laterality quotients for ^{18}F-flortaucipir BP_{ND} by performing one-way single-measure intra-class correlations across twin pairs. This reflects whether twins show similar hemispheric lateralization patterns of ^{18}F-flortaucipir BP_{ND}.

Second, for every participant, we extracted ^{18}F-flortaucipir BP_{ND} in each voxel from the MNI-space images with a grey matter mask overlayed. We correlated each participant's voxel-by-voxel ^{18}F-flortaucipir spatial distribution to that of every other participant using Spearman correlation models (Fig. 2A). This yielded 77 correlation coefficients for every participant (resulting in a 78 × 78 matrix of correlation coefficients) indicating how similar a participant's ^{18}F-flortaucipir spatial distribution is to that of every other participant. An independent *t*-test was performed to assess whether the average correlation coefficient obtained for twin pairs was significantly higher than the average correlation coefficient obtained for non-twin pairings of participants. This yields an estimate of whether twin pairs show a more similar ^{18}F-flortaucipir spatial distribution than non-twin pairs. To ensure that within-pair similarities in spatial distribution could not solely be explained by similarities in MNI-space warping parameters, we repeated the

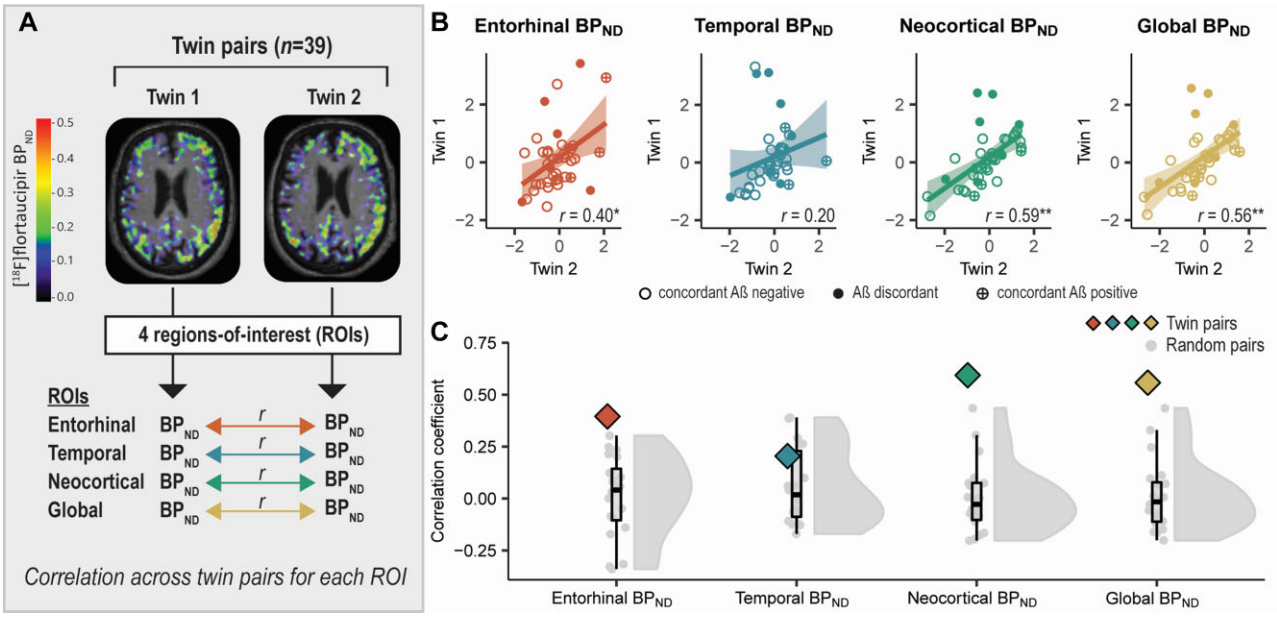

Figure 1 Identical twin pair correlations for global and regional ^{18}F-flortaucipir BP_{ND}. (**A**) For each region of interest, we performed age- and sex-adjusted one-way single-measure intra-class correlations across twin pairs (i.e. a correlation between Twin 1 and Twin 2 across the group) to examine within-pair similarities in ^{18}F-flortaucipir BP_{ND} (tau load). (**B**) Scatterplots illustrating twin-pair correlations in ^{18}F-flortaucipir BP_{ND} for each region of interest. Each dot represents a twin-pair. The values presented in the plots are the residuals of ^{18}F-flortaucipir BP_{ND} in Twin 1 (*y*-axis) and Twin 2 (*x*-axis) after regressing out the effects of age and sex. (**C**) The correlation coefficient observed for twin pairs (see **B**) is plotted against the distribution of correlation coefficients observed for random pairs. *P < 0.05; **P < 0.01.

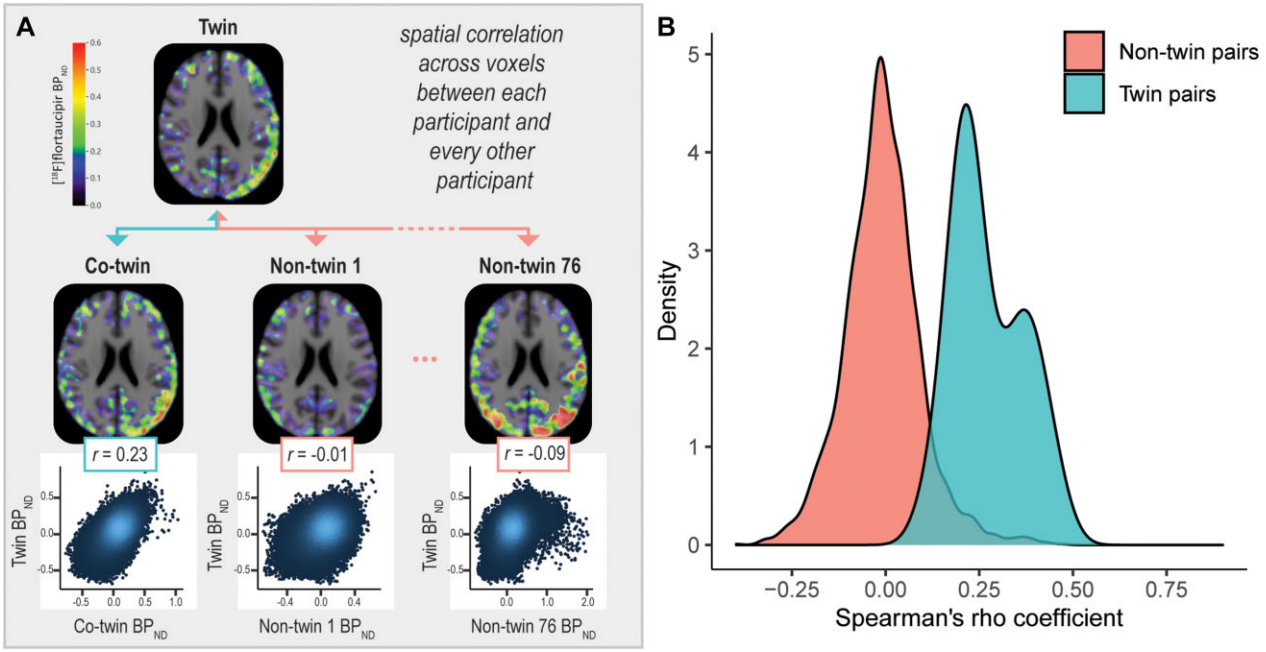

Figure 2 Spatial correlations for ^{18}F-flortaucipir PET between each participant and every other participant. (**A**) We correlated each participant's voxel-by-voxel ^{18}F-flortaucipir spatial distribution to that of every other participant using Spearman correlation models. (**B**) The distribution of spatial correlations (spearman's rho coefficient, corrected for age and sex) observed for twin pairs is compared against the distribution of spatial correlations observed for non-twin pairs.

analysis with subject-space brain regions from the Hammers template (including the same regions as included in the Braak III–IV and Braak V–VI regions of interest).

Last, we assessed whether we could successfully identify a participant's co-twin based on the strength of the previously established spatial correlation. If the highest correlation was observed for a participant's co-twin (instead of for a random other participant), it was considered a match. Otherwise, it was considered a miss. The success rate for twin pair identification was defined as the ratio between the number of matches and the total number of participants

$$[\text{success rate}(\%) = \frac{\sharp\,\text{matches}}{\sharp\,\text{participants}} \times 100] \quad (1)$$

As previous studies have postulated that cortical ^{18}F-flortaucipir signal in cognitively unimpaired elderly may be affected by off-target binding,[45] we performed sensitivity analyses in which we, for each cortical voxel, regressed out part of the signal that could be explained by off-target binding in the thalamus and putamen[45] using SPM12, to ensure that these results could not solely be explained by within-pair similarities in off-target binding.

Within twin-pair differences in BP_{ND} versus within twin-pair differences in environmental risk factors

We explored whether within-pair differences in ^{18}F-flortaucipir BP_{ND} were associated with within-pair differences in environmental risk factors using the within-identical twin pair difference model.[46] Specifically, we regressed the difference in regional ^{18}F-flortaucipir BP_{ND} in identical twin pairs on the difference in environmental risk factors in the same pair of twins corrected for age and sex. In a separate model, we additionally corrected for within-pair differences in global ^{18}F-flutemetamol BP_{ND} to explore whether observed associations were explained by within-pair differences in global amyloid-β load. Within-pair difference models with the DIN SRT score, a measure of hearing ability, were additionally corrected for hearing aid.

Data availability

The data that support the findings of this study are available from the corresponding author, upon reasonable request.

Results

Demographic characteristics and ^{18}F-flortaucipir BP_{ND} in each region of interest are summarized in Table 1. Seventy-eight participants (39 twin pairs) with an age of 73.4 ± 5.9 years were included in the analyses. Of the 78 participants, 40 (51.3%) carried an *APOE* ε4 allele and 15 (19.2%) were visually assessed as amyloid-β positive (4 years prior to tau-PET).

Mean ^{18}F-flortaucipir BP_{ND} was highest in the temporal (Braak III–IV) region of interest (Table 1). This was also observed in the group-average image of ^{18}F-flortaucipir BP_{ND}, revealing a predominant temporal binding pattern (Fig. 3). High ^{18}F-flortaucipir BP_{ND} was also observed in regions in the basal ganglia, typically known to be affected by off-target ^{18}F-flortaucipir binding.

Visual inspection of ^{18}F-flortaucipir PET

On visual inspection, we mostly observed similarities in twins in both the intensity as well as the distribution of ^{18}F-flortaucipir binding. However, dissimilarities in twins in ^{18}F-flortaucipir PET were also observed. Figure 4 shows ^{18}F-flortaucipir PET scans from four identical twin pairs showing similarities and two pairs showing

Table 1 Demographics

	Total sample
n	78 (39 pairs)
Age, years	73.4 ± 5.9
Female, *n* (%)	40 (51.3%)
Education, years	12.3 ± 2.9
MMSE score	28.7 ± 1.3
APOE ϵ4 positivity, *n* (%)	40 (51.3%)
Amyloid-β status, *n* positive (%)	15 (19.2%)
Global ^{18}F-flutemetamol BP_{ND}	0.18 ± 0.14[a]
Amyloid-β twin-pair status, *n* pairs	
Amyloid-β concordant negative	28 pairs
Amyloid-β discordant	7 pairs
Amyloid-β concordant positive	4 pairs
^{18}F-flortaucipir BP_{ND}	
Entorhinal (Braak I)	0.02 ± 0.14
Temporal (Braak III–IV)	0.10 ± 0.08
Neocortical (Braak V–VI)	0.04 ± 0.05
Global (Braak I–VI)	0.04 ± 0.05

Mean ± SD are reported unless stated otherwise. Age and Mini-Mental State Examination are measured at time of tau-PET; amyloid-β variables are from 4 years prior to tau-PET.
[a]Global ^{18}F-flutemetamol BP_{ND} was missing for four participants.

dissimilarities in ^{18}F-flortaucipir PET, that were selected for illustration purposes.

Twin pair similarities in global and regional ^{18}F-flortaucipir binding potential

In twins (corrected for effects of age and sex), global (Braak I–VI) ^{18}F-flortaucipir BP_{ND} correlated significantly ($r = 0.56$; $P < 0.01$) (Fig. 1B). Regionally, ^{18}F-flortaucipir BP_{ND} moderately correlated in twins in the entorhinal (Braak I) ($r = 0.40$; $P = 0.01$) and neocortical composite (Braak V–VI) ($r = 0.59$; $P < 0.01$) regions (Fig. 1B). The within-pair correlation for ^{18}F-flortaucipir BP_{ND} in the temporal composite (Braak III–IV) region, however, was non-significant ($r = 0.20$; $P = 0.10$) and fell within the range of what was found for random pairs (Fig. 1B and C). The correlation coefficient observed for twin pairs was significantly higher than the average correlation coefficient observed for random pairs for the entorhinal (*r* twin pairs: 0.40 versus average *r* random pairs: 0.01), neocortical composite (*r* twin pairs: 0.59 versus average *r* random pairs: 0.00) and global (*r* twin pairs: 0.56 versus average *r* random pairs: 0.01) regions, but not for the temporal composite region (*r* twin pairs: 0.20 versus average *r* random pairs: 0.06) (Fig. 1C).

We next explored the influence of baseline amyloid-β status on the observed within-pair correlations for ^{18}F-flortaucipir BP_{ND}. We observed that twin-pairs discordant on amyloid-β status 4 years prior to tau-PET (i.e. one twin being amyloid-β positive and the co-twin amyloid-β negative) often acted as outliers in the scatterplots (Fig. 1B). We therefore repeated the within-pair correlations after stratifying the sample based on discordant amyloid-β status ($n = 7$ pairs) or concordant amyloid-β status ($n = 32$ pairs). In amyloid-β concordant twins (corrected for effects of age and sex), ^{18}F-flortaucipir BP_{ND} was moderate-to-strongly correlated in all regions of interest, with strongest correlations observed in the neocortical composite ($r = 0.77$; $P < 0.01$) and global ($r = 0.75$; $P < 0.01$) regions, followed by the temporal composite ($r = 0.33$; $P = 0.03$) and entorhinal ($r = 0.48$; $P < 0.01$) regions (Supplementary Table 4). In contrast, in amyloid-β discordant twins, ^{18}F-flortaucipir BP_{ND} was not significantly correlated in any of the regions of interest (range *r*: 0.04–0.25; range *P*: 0.26–0.45) (Supplementary Table 4).

Twin pair similarities in spatial distribution of ^{18}F-flortaucipir binding potential

Next, we examined similarities in identical twin pairs in the spatial distribution of ^{18}F-flortaucipir BP_{ND}. First, within-pair similarities in spatial distribution were examined regionally with the laterality quotient. Hemispheric lateralization in regional ^{18}F-flortaucipir BP_{ND} was significantly correlated in twins in the temporal ($r = 0.58$; $P < 0.01$), neocortical ($r = 0.69$; $P < 0.01$) and global ($r = 0.69$; $P < 0.01$) regions. No correlation in twins was observed in entorhinal hemispheric lateralization of ^{18}F-flortaucipir ($r = 0.09$; $P = 0.28$) (Fig. 5).

Second, we correlated each participant's voxel-by-voxel ^{18}F-flortaucipir spatial distribution to that of every other participant (Fig. 2A). Correlations of ^{18}F-flortaucipir BP_{ND} across voxels were on average significantly higher for twin pairs [mean $r = 0.27$; standard deviation (SD) = 0.09] than for non-twin pairings (mean $r = -0.01$; SD = 0.10) ($P < 0.01$) (Fig. 2B). These results were not affected when correcting for proxies of cortical off-target binding (mean *r* for twin pairs: 0.27 ± 0.09 versus mean *r* for non-twin pairs: −0.01 ± 0.09) ($P < 0.01$) or when correlating ^{18}F-flortaucipir BP_{ND} across subject-space regions of interest instead of MNI-space voxels (mean *r* for twin pairs: 0.57 ± 0.23 versus mean *r* for non-twin pairs: −0.01 ± 0.33) ($P < 0.01$).

Last, based on the strength of the spatial voxel-wise correlation between participants, we assessed the success rate in identifying a participant's co-twin. For 85.9% of the subjects, the highest spatial correlation was observed for a participant's co-twin instead of for a random other participant (67/78 = 85.9%). Upon adjusting for proxies of cortical off-target binding, the success rate remained high at 83.3%.

Environmental risk factors associated with within-pair differences in binding potential

As we also observed differences in twins in ^{18}F-flortaucipir PET (Fig. 4), which can largely be attributed to non-shared, environmental (e.g. lifestyle) factors, we explored whether within-pair differences in global and regional ^{18}F-flortaucipir BP_{ND} were associated with within-pair differences in environmental risk factors. Corrected for age and sex, within-pair differences in ^{18}F-flortaucipir BP_{ND} were associated with within-pair differences in GDS total score ($0.37 < \beta < 0.56$; $P < 0.05$, depending on the region of interest), within-pair differences in social activity ($-0.32 < \beta < -0.36$; $P < 0.05$, depending on the region of interest) and within-pair differences in PASE total score ($-0.41 < \beta < -0.42$; $P < 0.05$ depending on the region of interest) (Fig. 6 and Supplementary Table 5). Specifically, the twin with a higher ^{18}F-flortaucipir BP_{ND} also had more depressive symptoms, more strongly affected social activity and less physical activity. Upon additionally correcting the within-pair difference regression models for within-pair differences in global ^{18}F-flutemetamol BP_{ND}, within-pair differences in entorhinal ^{18}F-flortaucipir BP_{ND} remained associated with within-pair differences in GDS total score ($\beta = 0.39$; $P = 0.02$), and within-pair differences in entorhinal and temporal ^{18}F-flortaucipir BP_{ND} remained associated with within-pair differences in PASE total score ($\beta = 0.40$; $P = 0.01$ and $\beta = 0.33$; $P = 0.02$, respectively). Effect sizes and corresponding *P*-values are shown in Supplementary Table 5.

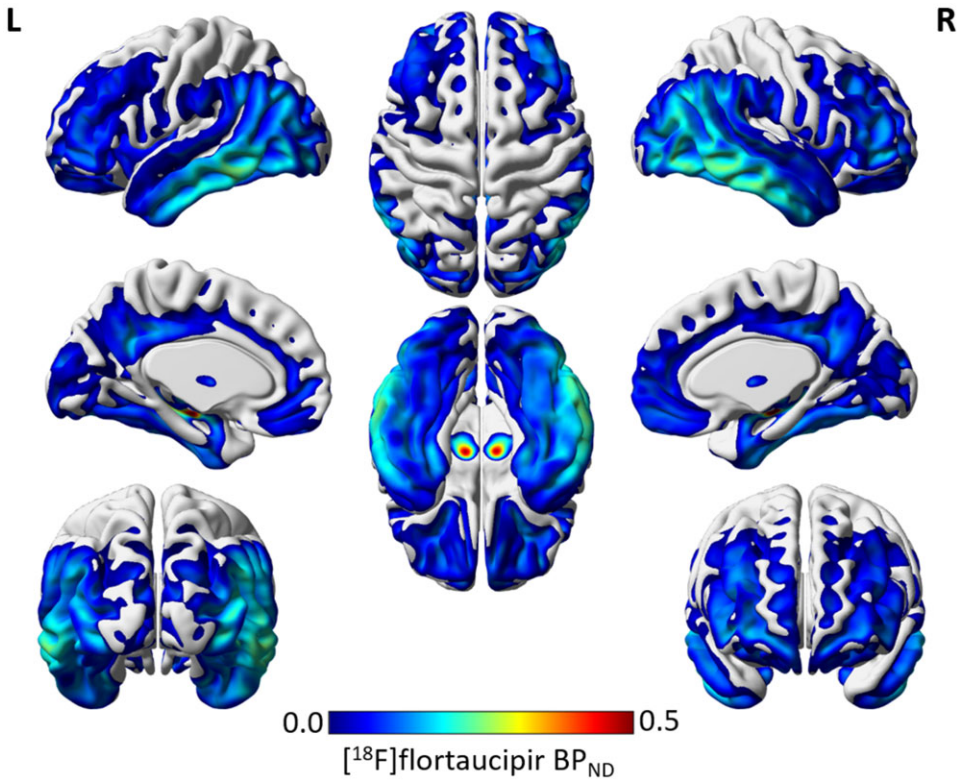

Figure 3 Group average image of ^{18}F-flortaucipir BP_{ND}.

Discussion

In this study, we examined similarities and dissimilarities in genetically identical cognitively unimpaired older twins in load and spatial distribution of tau pathology measured with ^{18}F-flortaucipir PET. We observed substantial within-pair similarities in tau pathology load, voxel-wise spatial distribution and asymmetry measures. Based on the spatial distribution of tau pathology, we could identify which twins belonged to the same pair with an accuracy of 86%. These results suggest genetic factors to play an important role in the earliest increases and spatial patterns of tau pathology. However, dissimilarities in twins in tau PET were also observed, indicating a potential role for (possibly modifiable) environmental factors in secondary prevention.

One of the main findings in the present study was that global and regional tau PET load were significantly correlated in twins, and twins of the same twin pair were significantly more alike in their tau PET load than random paired twin individuals, also after adjusting for potential age- and sex-effects. This is in line with our earlier study,[41] in which we observed within-pair similarities in cerebrospinal fluid tau pathology of similar strength as to what we currently observed using PET imaging. Observations from post-mortem human brains of monozygotic twins with and without diagnosis of clinical Alzheimer's disease dementia have indicated both within-pair concordances[47] as well as within-pair discordances[48] in neurofibrillary tau tangle Braak staging. These results suggest that the susceptibility to and initial development of pathology may be genetically determined, but genetics alone may not be sufficient to determine the complete pathological and clinical course of the disease.

We observed moderate-to-strong within-pair correlations for regional tau pathology in the entorhinal and neocortical composite region, but a substantial weaker and non-significant correlation in the temporal composite region. The moderate within-pair correlation in the entorhinal cortex, one of the brain sites in the medial temporal lobe in which neurofibrillary tangles appear first,[8,9] suggests genetic factors to influence the earliest increases of tau pathology. Tau tangles in the medial temporal lobe in cognitively unimpaired individuals have previously been associated with subtle cognitive deficits and longitudinal cognitive decline,[15,21–23] even when tau-tracer binding is lower than observed in clinical Alzheimer's disease, and therefore do not seem to be benign. Whether or not a genetic predisposition to the earliest increases in entorhinal tau translates to a risk for future clinical progression needs further investigation. The within-pair correlation in the temporal composite region (Braak III–IV) was affected by some twin pairs acting as outliers in the analysis. Interestingly, upon further inspection, we noted that the twin pairs that acted as outliers—and thus were dissimilar in their temporal tau-PET BP_{ND}—were often also discordant on their baseline amyloid-β status, meaning one twin being amyloid-β positive and the co-twin being amyloid-β negative based on PET visual read. Repeating the analysis while excluding the amyloid-β discordant twin pairs indeed led to a strengthening of the within-pair correlation in temporal BP_{ND}. Studies have indicated that tau pathology beyond the medial temporal lobe is typically accompanied with the presence of cortical amyloid-β pathology,[49] which has led to the hypothesis that amyloid-β plays a key factor in the spread of tau outside of the medial temporal lobe. Our results are in line with this hypothesis, as within-pair similarities in twins in the temporal composite region (including lateral temporal regions) became stronger and significant when amyloid-β discordant twins were excluded, although it is notable that the within-pair correlation in the temporal region remained considerably weaker than that of the other brain regions,

suggesting a role for other factors (or mechanisms) as well. Following the same hypothesis, it would have been expected that this would also affect the within-pair correlation in neocortical tau pathology. Instead, we observed a strong within-pair correlation for neocortical tau, exceeding levels of similarity that could have been obtained by chance. However, cautious interpretation is needed for the within-pair correlation in neocortical tau, as the BP_{ND} are all in the very low range. A cohort also consisting of twin pairs with clinically manifest Alzheimer's disease might be preferred to infer conclusions on similarities in tau pathology in late-stage tau.

Our data suggest that not only early tau load is under genetic influence, but also the regional localization of tau. Although the amount of preclinical Alzheimer's disease tau pathology is overall low (for comparison, in the current study we observed a Braak III–IV BP_{ND} of 0.1 ± 0.1, whereas we previously observed a BP_{ND} of 0.4 ± 0.2 in clinical Alzheimer's disease[50]), we observed strong similarities in pairs in asymmetric deposition of tau within larger cortical regions. Asymmetric tau deposition is a characteristic feature in atypical Alzheimer's disease phenotypes, but some degree of lateralization also exists in typical Alzheimer's disease.[7,13,14] The absence of a strong within-pair correlation in temporal tau BP_{ND} combined with the presence of a strong within-pair correlation in temporal tau laterality quotient may indicate that genetic factors influence the brain's regional vulnerability to tau pathology, but external factors (among which amyloid-β, vascular components or lifestyle factors) that are unique to a twin may influence the actual accumulation of tau. This is corroborated by our voxel-wise analyses, indicating that the voxel-wise pattern of tau pathology was significantly more similar between twins of the same pair compared to twins of random pairs, and that even though some twin pairs were discordant for amyloid-β status, we could identify a twin solely based on the spatial correlation with its co-twin in approximately nine out of 10 pairs. The pathway through which genetic factors may influence the regional localization of tau pathology remains to be further examined, though recent *in vivo* PET studies support a role of brain connectivity patterns in the spread of tau throughout the brain.[13,51–54] Whether the association between brain connectivity and tau spread throughout the brain is influenced by shared underlying genetic mechanisms, for example via the influence of genetics on cortical patterning and hub connectivity,[55,56] would be of interest for future twin projects.

Although the results of this study mainly reveal similarities in tau PET characteristics in twin pairs, there were also twin pairs that showed strong dissimilarities in tau PET of which two are highlighted in Fig. 2. A major question remains which factors can explain the differences in tau pathology that we observed in twin pairs that are genetically identical. Our data suggest that differences in amyloid-β pathology are likely associated with the observed differences in tau, and this should be examined in more detail. We found that within-pair differences in tau pathology were associated with within-pair differences in depressive symptoms, social activity and physical activity. Interestingly, the

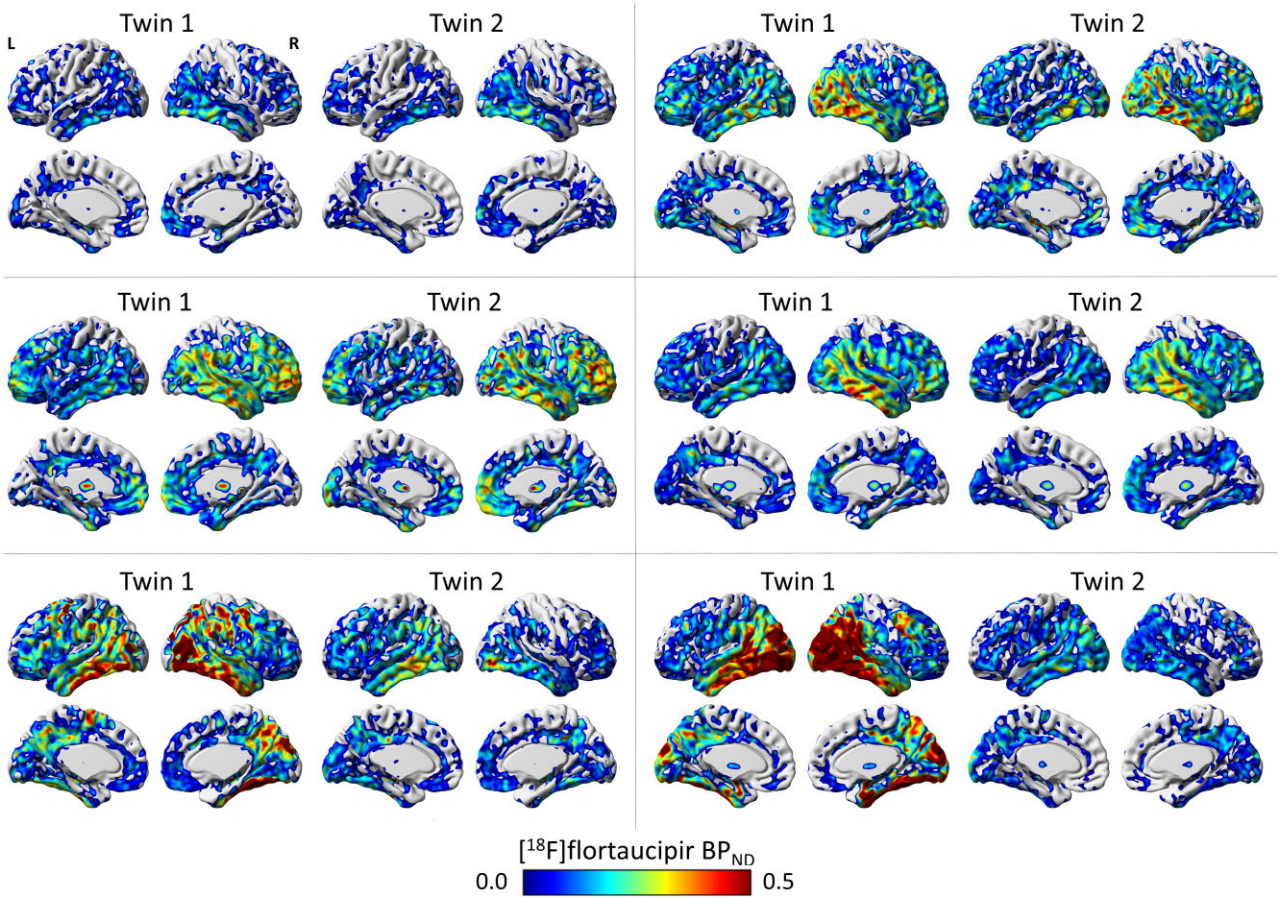

Figure 4 Examples of ^{18}F-flortaucipir PET scans from six genetically identical twin pairs. Shown are the ^{18}F-flortaucipir PET scans from six genetically identical twin pairs. For illustration purposes, we selected pairs that show within-pair similarities in ^{18}F-flortaucipir BP_{ND} and distribution (*top* and *middle* row), as well as within-pair dissimilarities (*bottom* row).

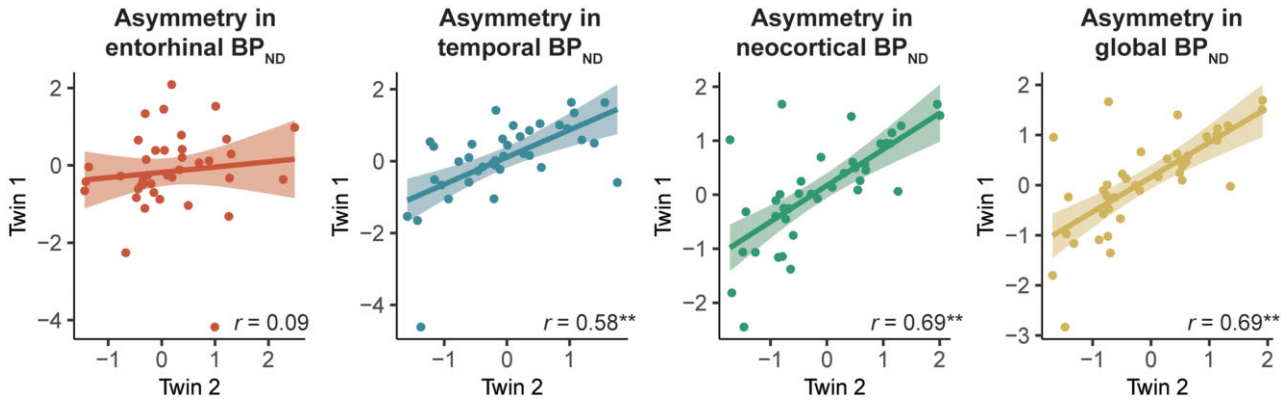

Figure 5 Identical twin pair correlations for hemispheric lateralization in global and regional ^{18}F-flortaucipir BP$_{ND}$. Shown are the scatterplots illustrating the twin-pair associations in regional laterality quotients for ^{18}F-flortaucipir BP$_{ND}$. Each dot represents a twin-pair. The values presented in the plots are the residuals of the laterality quotient in regional and global ^{18}F-flortaucipir BP$_{ND}$ for Twin 1 (y-axis) and Twin 2 (x-axis) after regressing out the effects of age and sex. *$P < 0.05$; **$P < 0.01$.

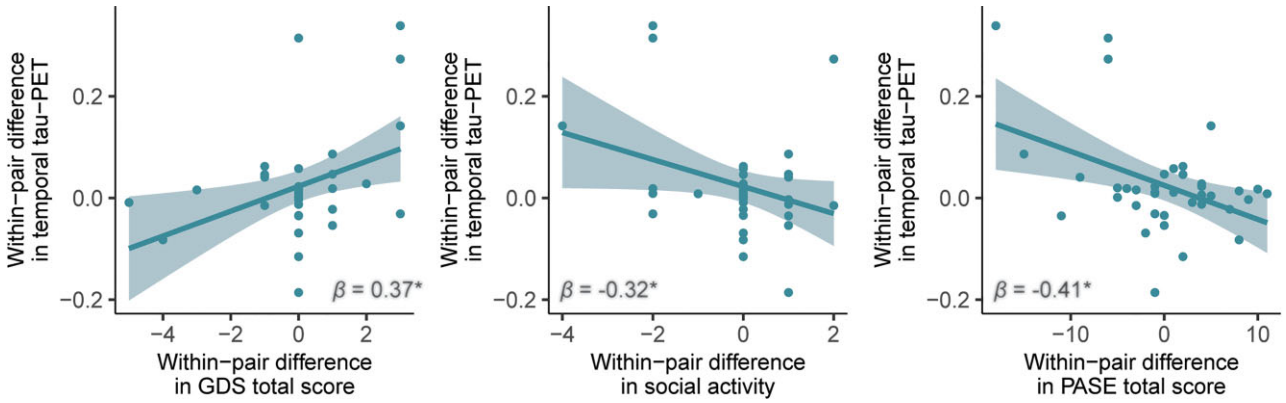

Figure 6 Within twin-pair differences regression models between within-pair differences in ^{18}F-flortaucipir BP$_{ND}$ and within-pair differences in Geriatric Depression Scale total score, social activity and Physical Activity Scale for the Elderly total score. Each dot represents a twin-pair. Values presented in the plots represent the raw difference in temporal ^{18}F-flortaucipir BP$_{ND}$ between Twin 1 and Twin 2 for each pair (y-axis), and the raw differences in GDS total score, social activity and PASE total score between Twin 1 and Twin 2 for each pair (x-axis). Reported β and *P*-values are from age and sex-corrected regression models. *$P < 0.05$.

observed associations between within-pair differences in tau pathology and within-pair differences in depressive symptoms and physical activity were partly independent of within-pair differences in global amyloid-β load. Although unable to establish causality due to the cross-sectional design of the current study, these findings are interesting given that previous studies have also linked resistance to Alzheimer's disease pathology (lower levels of pathology than expected)[57] with lifestyle factors including physical activity.[58,59] However, as the environmental risk factor variables in the current study were measured at time of tau-PET, it is not possible to conclude whether these are upstream or downstream effects of Alzheimer's disease pathology.

Future longitudinal twin studies will be of interest for several reasons. First, longitudinal data may enable investigation of possible causal relationships between environmental (e.g. lifestyle) risk factors, which may be potentially modifiable, Alzheimer's disease pathology and cognitive decline. Second, longitudinal twin data is needed to clarify whether twins who are currently different for Alzheimer's disease pathology (i.e. one twin having more pathology than the co-twin), may over time become similar, or whether they remain different—and thus whether it is a matter of a difference in disease development or a difference in the timing of disease onset. Understanding which, potentially modifiable, environmental factors are associated with either the complete absence or a delay in the onset and spread of tau pathology would be of great importance for prevention strategies.

This study had some limitations. Firstly, we only included genetically identical twin pairs, while classic twin studies include both genetically identical and fraternal twins, that share on average half of their segregating genes. By not including fraternal twins, we could not disentangle genetic from shared environmental influences. Secondly, our study was limited by a relatively small sample size. Thirdly, a general limitation when studying preclinical Alzheimer's disease pathology is that the overall levels of tau pathology are relatively low. Fourthly, second-generation tau tracers may be preferred to examine tau pathology in the earliest stages of the Alzheimer's disease continuum because of less off-target binding in the hippocampus, a region in which tau accumulation occurs early in the disease process.[8,9] Last, results are based on cross-sectional data only, and longitudinal data will be needed to examine whether the within-pair similarities may differ over time.

Conclusion

Our results indicate that genetically identical twins show substantial similarities in load, spatial distribution and asymmetry

measures of tau pathology, supportive of an important role for genetic factors in the earliest stages of Alzheimer's disease. However, considering also the presence of dissimilarities in tau pathology in twin pairs, genetics alone are likely insufficient to explain the complete pathological course of the disease.

Acknowledgements

We kindly thank all participating twins for their dedication. Research of Amsterdam Alzheimer Center is part of the Neurodegeneration program of Amsterdam Neuroscience. The Amsterdam Alzheimer Center is supported by Alzheimer Nederland and Stichting VUmc funds. ^{18}F-Flortaucipir PET scans were made possible by Avid Radiopharmaceuticals Inc.

Funding

This study was made possible by the EU/European Federation of Pharmaceutical Industries and Associations Innovative Medicines Initiative Joint Undertaking (EMIF grant 115372), the Grand Prix of the Association for Research on Alzheimer Disease, Alzheimer Nederland and ZonMW. This project has received funding from the Innovative Medicines Initiative 2 Joint Undertaking under grant agreement No 115952. This Joint Undertaking receives support from the European Union's Horizon 2020 research and innovation program and EFPIA. This communication reflects the views of the authors and neither IMI nor the European Union and EFPIA are liable for any use that may be made of the information contained herein.

Competing interests

E.M.C., J.T., R.O., S.S.V.G., M.H., L.E.C., E.W., S.L., E.E.W., E.J.C.G. and A.B. report no competing interests. A.D.W. is editor-in-chief of Nuclear Medicine and Biology. F.B. is supported by the NIHR UCLH biomedical research centre. F.B. is supported by the European Union's Horizon 2020 research and innovation programme under grant agreement No. 666992. P.S. has received consultancy fees (paid to the institution) from AC Immune, Biogen, Brainstorm Cell, EIP, ImmunoBrain Checkpoint, Genentech, Novartis, Novo Nordisk. He is PI of studies with AC Immune, CogRx, FUJI-film/Toyama, UCB and Vivoryon. He is a part-time employee of Life Sciences Partners Amsterdam. He serves on the board of Brain Research Center and New Amsterdam Pharma. P.J.V. received nonfinancial support from GE Healthcare, research support from Biogen and grants from EU/EFPIA Innovative Medicines Initiative Joint Undertaking, EU Joint Programme–Neurodegenerative Disease Research (JPND and ZonMw). B.N.M.B. received research support from ZonMW, AVID radiopharmaceuticals, CTMM and Janssen Pharmaceuticals. He is a trainer for Piramal and GE. He receives no personal honoraria.

Supplementary material

Supplementary material is available at *Brain* online.

References

1. Sperling RA, Aisen PS, Beckett LA, *et al*. Toward defining the preclinical stages of Alzheimer's disease: recommendations from the National Institute on Aging-Alzheimer's Association workgroups on diagnostic guidelines for Alzheimer's disease. *Alzheimers Dement*. 2011;7(3):280–292.
2. Jansen WJ, Ossenkoppele R, Knol DL, *et al*. Prevalence of cerebral amyloid pathology in persons without dementia: a meta-analysis. *JAMA*. 2015;313(19):1924–1938.
3. Jack C Jr, Holtzman DM. Biomarker modeling of Alzheimer's disease. *Neuron*. 2013;80(6):1347–1358.
4. Harrison TM, La Joie R, Maass A, *et al*. Longitudinal tau accumulation and atrophy in aging and alzheimer disease. *Ann Neurol*. 2019;85(2):229–240.
5. Lehmann M, Ghosh PM, Madison C, *et al*. Diverging patterns of amyloid deposition and hypometabolism in clinical variants of probable Alzheimer's disease. *Brain*. 2013;136(Pt 3):844–858.
6. Johnson KA, Schultz A, Betensky RA, *et al*. Tau positron emission tomographic imaging in aging and early Alzheimer disease. *Ann Neurol*. 2016;79(1):110–119.
7. Vogel JW, Young AL, Oxtoby NP, *et al*. Four distinct trajectories of tau deposition identified in Alzheimer's disease. *Nat Med*. 2021;27(5):871–881.
8. Braak H, Braak E. Neuropathological stageing of Alzheimer-related changes. *Acta Neuropathol*. 1991;82(4):239–259.
9. Braak H, Braak E. Staging of Alzheimer's disease-related neurofibrillary changes. *Neurobiol Aging*. 1995;16(3):271–278; discussion 278–84.
10. Cho H, Choi JY, Hwang MS, *et al*. In vivo cortical spreading pattern of tau and amyloid in the Alzheimer disease spectrum. *Ann Neurol*. 2016;80(2):247–258.
11. Schöll M, Lockhart SN, Schonhaut DR, *et al*. PET Imaging of tau deposition in the aging human brain. *Neuron*. 2016;89(5):971–982.
12. Schwarz AJ, Yu P, Miller BB, *et al*. Regional profiles of the candidate tau PET ligand 18F-AV-1451 recapitulate key features of Braak histopathological stages. *Brain*. 2016;139(Pt 5):1539–1550.
13. Vogel JW, Iturria-Medina Y, Strandberg OT, *et al*. Spread of pathological tau proteins through communicating neurons in human Alzheimer's disease. *Nat Commun*. 2020;11(1):2612.
14. Ossenkoppele R, Schonhaut DR, Schöll M, *et al*. Tau PET patterns mirror clinical and neuroanatomical variability in Alzheimer's disease. *Brain*. 2016;139(Pt 5):1551–1567.
15. Hanseeuw BJ, Betensky RA, Jacobs HIL, *et al*. Association of amyloid and tau with cognition in preclinical Alzheimer disease: A longitudinal study. *JAMA Neurol*. 2019;76:915.
16. Ossenkoppele R, Smith R, Ohlsson T, *et al*. Associations between tau, Aβ, and cortical thickness with cognition in Alzheimer disease. *Neurology*. 2019;92(6):e601–e612.
17. Harrison TM, Du R, Klencklen G, Baker SL, Jagust WJ. Distinct effects of beta-amyloid and tau on cortical thickness in cognitively healthy older adults. *Alzheimers Dement*. 2020;17:1085–1096.
18. Aschenbrenner AJ, Gordon BA, Benzinger TLS, Morris JC, Hassenstab JJ. Influence of tau PET, amyloid PET, and hippocampal volume on cognition in Alzheimer disease. *Neurology*. 2018;91(9):e859–e866.
19. Bejanin A, Schonhaut DR, La Joie R, *et al*. Tau pathology and neurodegeneration contribute to cognitive impairment in Alzheimer's disease. *Brain*. 2017;140(12):3286–3300.
20. Visser D, Wolters EE, Verfaillie SCJ, *et al*. Tau pathology and relative cerebral blood flow are independently associated with cognition in Alzheimer's disease. *Eur J Nucl Med Mol Imaging*. 2020;47(13):3165–3175.
21. Maass A, Lockhart SN, Harrison TM, *et al*. Entorhinal tau pathology, episodic memory decline, and neurodegeneration in aging. *J Neurosci*. 2018;38(3):530–543.
22. Lowe VJ, Bruinsma TJ, Wiste HJ, *et al*. Cross-sectional associations of tau-PET signal with cognition in cognitively unimpaired adults. *Neurology*. 2019;93(1):e29–e39.

23. Sperling RA, Mormino EC, Schultz AP, *et al*. The impact of amyloid-beta and tau on prospective cognitive decline in older individuals. *Ann Neurol*. 2019;85(2):181–193.
24. Kremen WS, Prom-Wormley E, Panizzon MS, *et al*. Genetic and environmental influences on the size of specific brain regions in midlife: the VETSA MRI study. *Neuroimage*. 2010;49(2):1213–1223.
25. Posthuma D, de Geus EJ, Neale MC, *et al*. Multivariate genetic analysis of brain structure in an extended twin design. *Behav Genet*. 2000;30(4):311–319.
26. Gatz M, Reynolds CA, Fratiglioni L, *et al*. Role of genes and environments for explaining Alzheimer disease. *Arch Gen Psychiatry*. 2006;63(2):168–174.
27. Konijnenberg E, Carter SF, Ten Kate M, *et al*. The EMIF-AD PreclinAD study: study design and baseline cohort overview. *Alzheimers Res Ther*. 2018;10(1):75.
28. Collij LE, Konijnenberg E, Reimand J, *et al*. Assessing amyloid pathology in cognitively normal subjects using (^{18})F-flutemetamol PET: Comparing visual reads and quantitative methods. *J Nucl Med*. 2019;60(4):541–547.
29. Collij LE, Heeman F, Salvado G, *et al*. Multitracer model for staging cortical amyloid deposition using PET imaging. *Neurology*. 2020;95(11):e1538–e1553.
30. Morris JC. The clinical dementia rating (CDR): current version and scoring rules. *Neurology*. 1993;43(11):2412–2414.
31. Morris JC, Heyman A, Mohs RC, *et al*. The consortium to establish a registry for Alzheimer's disease (CERAD). Part I. Clinical and neuropsychological assessment of Alzheimer's disease. *Neurology*. 1989;39(9):1159–1165.
32. Yesavage JA, Brink TL, Rose TL, *et al*. Development and validation of a geriatric depression screening scale: a preliminary report. *J Psychiatr Res*. 1982;17(1):37–49.
33. Tuncel H, Visser D, Yaqub M, *et al*. Effect of shortening the scan duration on quantitative accuracy of (^{18})F-flortaucipir studies. *Mol Imaging Biol*. 2021;23:604–613.
34. Hammers A, Allom R, Koepp MJ, *et al*. Three-dimensional maximum probability atlas of the human brain, with particular reference to the temporal lobe. *Hum Brain Mapp*. 2003;19(4):224–247.
35. Svarer C, Madsen K, Hasselbalch SG, *et al*. MR-based automatic delineation of volumes of interest in human brain PET images using probability maps. *Neuroimage*. 2005;24(4):969–979.
36. Golla SSV, Wolters EE, Timmers T, *et al*. Parametric methods for (^{18})F-flortaucipir PET. *J Cereb Blood Flow Metab*. 2020;40(2):365–373.
37. Golla SSV, Lubberink M, van Berckel BNM, Lammertsma AA, Boellaard R. Partial volume correction of brain PET studies using iterative deconvolution in combination with HYPR denoising. *EJNMMI Res*. 2017;7(1):36.
38. Ossenkoppele R, Rabinovici GD, Smith R, *et al*. Discriminative accuracy of 18F-flortaucipir positron emission tomography for alzheimer disease vs other neurodegenerative disorders. *JAMA*. 2018;320(11):1151–1162.
39. Wolters EE, Golla SSV, Timmers T, *et al*. A novel partial volume correction method for accurate quantification of (^{18})F- flortaucipir in the hippocampus. *EJNMMI Res*. 2018;8(1):79.
40. Oldfield RC. The assessment and analysis of handedness: the Edinburgh inventory. *Neuropsychologia*. 1971;9(1):97–113.
41. Konijnenberg E, Tomassen J, den Braber A, *et al*. Onset of preclinical Alzheimer disease in monozygotic twins. *Ann Neurol*. 2021;89:987–1000.
42. Livingston G, Huntley J, Sommerlad A, *et al*. Dementia prevention, intervention, and care: 2020 report of the Lancet Commission. *Lancet*. 2020;396(10248):413–446.
43. Smits C, Theo Goverts S, Festen JM. The digits-in-noise test: assessing auditory speech recognition abilities in noise. *J Acoust Soc Am*. 2013;133(3):1693–1706.
44. Washburn RA, Smith KW, Jette AM, Janney CA. The physical activity scale for the elderly (PASE): development and evaluation. *J Clin Epidemiol*. 1993;46(2):153–162.
45. Baker SL, Harrison TM, Maass A, La Joie R, Jagust WJ. Effect of off-target binding on (18)F-flortaucipir variability in healthy controls across the life span. *J Nucl Med*. 2019;60(10):1444–1451.
46. De Moor MHM, Boomsma DI, Stubbe JH, Willemsen G, de Geus EJ. Testing causality in the association between regular exercise and symptoms of anxiety and depression. *Arch Gen Psychiatry*. 2008;65(8):897–905.
47. Brickell KL, Leverenz JB, Steinbart EJ, *et al*. Clinicopathological concordance and discordance in three monozygotic twin pairs with familial Alzheimer's disease. *J Neurol Neurosurg Psychiatry*. 2007;78(10):1050–1055.
48. Iacono D, Volkman I, Nennesmo I, *et al*. Neuropathologic assessment of dementia markers in identical and fraternal twins. *Brain Pathol*. 2014;24(4):317–333.
49. Bennett RE, DeVos SL, Dujardin S, *et al*. Enhanced tau aggregation in the presence of amyloid beta. *Am J Pathol*. 2017;187(7):1601–1612.
50. Wolters EE, Ossenkoppele R, Verfaillie SCJ, *et al*. Regional (^{18})F-flortaucipir PET is more closely associated with disease severity than CSF p-tau in Alzheimer's disease. *Eur J Nucl Med Mol Imaging*. 2020;47(12):2866–2878.
51. Ossenkoppele R, Iaccarino L, Schonhaut DR, *et al*. Tau covariance patterns in Alzheimer's disease patients match intrinsic connectivity networks in the healthy brain. *Neuroimage Clin*. 2019;23:101848.
52. Cope TE, Rittman T, Borchert RJ, *et al*. Tau burden and the functional connectome in Alzheimer's disease and progressive supranuclear palsy. *Brain*. 2018;141(2):550–567.
53. Franzmeier N, Rubinski A, Neitzel J, *et al*. Functional connectivity associated with tau levels in ageing. Alzheimer's, and small vessel disease. *Brain*. 2019;142(4):1093–1107.
54. Jacobs HIL, Hedden T, Schultz AP, *et al*. Structural tract alterations predict downstream tau accumulation in amyloid-positive older individuals. *Nat Neurosci*. 2018;21(3):424–431.
55. Schmitt JE, Neale MC, Fassassi B, *et al*. The dynamic role of genetics on cortical patterning during childhood and adolescence. *Proc Natl Acad Sci USA*. 2014;111(18):6774–6779.
56. Arnatkeviciute A, Fulcher BD, Oldham S, *et al*. Genetic influences on hub connectivity of the human connectome. *Nat Commun*. 2021;12(1):4237.
57. Arenaza-Urquijo EM, Vemuri P. Resistance vs resilience to Alzheimer disease: Clarifying terminology for preclinical studies. *Neurology*. 2018;90(15):695–703.
58. Okonkwo OC, Schultz SA, Oh JM, *et al*. Physical activity attenuates age-related biomarker alterations in preclinical AD. *Neurology*. 2014;83(19):1753–1760.
59. Schreiber S, Vogel J, Schwimmer HD, Marks SM, Schreiber F, Jagust W. Impact of lifestyle dimensions on brain pathology and cognition. *Neurobiol Aging*. 2016;40:164–172.